Synthesis of 2D-CZTS Nanoplate as Photocathode Material for Efficient PEC Water Splitting

V. Mahalakshmi
Gobi Arts and Science College

Venugopal D (venu@gascgobi.ac.in)
Gobi Arts and Science College https://orcid.org/0000-0001-8330-3282

K. Ramachandran
Periyar University

R. Ramesh
Periyar University

Original Research

Keywords: Photocathode, Cu2ZnSnS4, Water splitting, 2D nanoplate, Annealing time

Posted Date: February 12th, 2021

DOI: https://doi.org/10.21203/rs.3.rs-187634/v1

Version of Record: A version of this preprint was published at Journal of Materials Science: Materials in Electronics on July 29th, 2021. See the published version at https://doi.org/10.1007/s10854-021-06400-9.

Synthesis of 2D-CZTS nanoplate as photocathode material for efficient PEC water splitting

V.Mahalakshmi[a], D.Venugopal[a*], K.Ramachandran[b], R.Ramesh[b]

[a]Department of Physics, Gobi Arts & Science College, Gobichettipalayam -638453, Tamilnadu, India.

[b]Department of Physics, Periyar University, Salem-11, Tamil Nadu, India.

Corresponding author E-mail: venu@gascgobi.ac.in

ABSTRACT

Fabrication of economically viable photocathode for hydrogen energy production through solar water splitting is a major research among the scientific community for a decade. P-type compound Cu_2ZnSnS_4 (CZTS) is very interesting material due to its absorption property, earth-abundant constituents and environmental friendliness that serves as a suitable candidate to act as a photocathode. In the present work, Cu_2ZnSnS_4 (CZTS) nanoparticles are synthesized by simple one-step chemical method and annealed at 350 °C for three different times (60 minutes, 90 minutes and 120 minutes). The effect of annealing time on the structural, optical and photoelectrochemical properties are investigated. XRD pattern indicates the formation of tetragonal crystal structure and the crystallinity increases according to the annealing time. 2-D nanoplate morphology is obtained for the sample that was annealed for 120 minutes. From the absorption spectra, it was found that the band gap decreases with increase of annealing time. Further, the prepared nanoparticle thin films are used as a cathode for photoelectrochemical water splitting application. Among these, the nanoparticles that are annealed for 120 minutes showed higher photocurrent density when compared to nanoparticles annealed for 60 minutes and 90 minutes.

Keywords: Photocathode, Cu_2ZnSnS_4, Water splitting, 2D nanoplate, Annealing time

1. INTRODUCTION

Renewable energy resources procure substantial involvement in the area of alternative source of energy [1] and is seen as an best solution for addressing the current and future energy demands of our human society. Therefore working and exploring in the field of new materials is necessary to achieve the goal of cost-effective one, for example converting solar

energy into electrical energy via photoelectrochemical reactions, photovoltaic and photocatalytic technology [2]. The most promising and emerging technology for converting solar energy into electrical energy is photocatalytic and electrocatalytic water splitting. Natural photosynthesis is inefficient because it captures less number of photons, so charge separation and charge transfer are limited. But artificial photosynthesis is a novel technology, which converts light energy (solar energy) into chemical energy by using semiconductors as photocatalysts. Also, it is an alternative for the natural process as it captures more photons and increase the charge transportation. The main aim of artificial photosynthesis is to capture more sunlight and split the water molecules to produce renewable energy (hydrogen fuel). Hydrogen (H_2) is a clean fuel and it emits water upon utilization and it does not emit greenhouse gases, free from air pollution[3]. With the existing production mechanisms, cost and the under-developed technology, utilization of hydrogen fuel has many practical difficulties. To overcome such difficulties, wide knowledge is required in theoretical and experimental research. Recently, many researchers have been devoid of green and sustainable technology towards the clean environment for the production of hydrogen fuel through photocatalytic (PC) and photoelectrochemical (PEC) water splitting. The major hurdle in these methods is the evolution of a suitable semiconductor-based photocatalyst with good light-absorption properties in the visible region[4].

Photoelectrochemical (PEC) water splitting is a complex process because,efficient device design and several phenomena must be optimized. The most fundamental ones are the interaction of light with matter, generation of electron-hole pairs, separation of charge and its transport, transfer of charge from the catalyst to electrolyte and the water-splitting reaction. A current flow is obtained between both the electrodes, when the water splitting occurs [5]. For PEC, numerous photoanodes (n-type semiconductors) have been investigated for water oxidation. However, relatively few work has been carried out on the photocathodes (p-type semiconductors) for water reduction[6,7]. The recent research in (PEC) water splitting is focused on p-type semiconductor including oxides and sulphides, which has received more attention than that of p-type silicon and III-V semiconductor photocathodes. To have a large photocurrent density, the conduction band edge potential of photocathode material needs to be more negative than the hydrogen redox potential in PEC.

Materials with direct bandgap energies in the range of 1-2eV acquire maximum light absorption from the solar spectrum[8] because, direct bandgap materials absorb light quickly before it goes deeper into the absorbing material compared to indirect bandgap materials. Copper Zinc Tin Sulphide (CZTS) is a good substitute for present photovoltaic and

photocatalytic materials[9–11]. CZTS is better than Copper Indium Selenium (CIS) and copper indium gallium selenide (CIGS) since it is composed of scarce, expensive, and relatively toxic materials. CZTS is a p-type quaternary semiconductor compound with the kesterite crystal structure. The components in CZTS are rich in the earth's crust and it is harmless, economic, and non-hazardous[12–14]. It is a potential material for the photovoltaic absorber layer with direct bandgap energy of 1.4eV – 1.6eV and absorption coefficient $\square 10^4$ cm^{-1} in the visible region [15]. The first report of CZTS-based photocathode for hydrogen production was reported by Yokoyama et al., [16]. Zhang et al., synthesize CZTS photocathodes via electrodeposition of metal precursors followed by sulfurization [17]. The recent approach for the development and optimization of the photocathodes for PEC water spitting, motivate to investigate this favourable photocathode material for PEC energy conversion.

The focus of present work was the preparation of CZTS nanoparticles by simple one-step chemical method using non-toxic solvent water. Because most organic and inorganic mixures can favorably dissolved in water. CZTS nanoparticles are synthesized at an annealing temperature of 350°C with different annealing times. In order to optimize the annealing time for a particular annealing temperature, structural, morphological, and optical properties are investigated. The PEC performance of CZTS nanoparticle thin films are studied by fabricating CZTS photocathode, to find its appropriateness for water splitting applications.

2. EXPERIMENTAL DETAILS

2.1. Materials

$CuCl_2.2H_2O$ - Copper(II)Chloride Dihydrate, $ZnCl_2$ - Zinc Chloride, $SnCl_2.2H_2O$ - Tin(II)Chloride Dihydrate and H_2NCSNH_2 - Thiourea are the starting materials used without further purification.

2.2. Preparation of CZTS nanoparticles

CZTS nanoparticles have been synthesized through a simple one-step chemical method. 1M of $CuCl_2.2H_2O$, 0.5M of $ZnCl_2$, 0.5M of $SnCl_2.2H_2O$ and 2M of H_2NCSNH_2 are dissolved in 40ml of double distilled water for the preparation of the initial solution. To dissolve the components completely, the solution was stirred on a magnetic stirrer for 1 hour at 60 °C. The precipitates are washed several times using ethanol and distilled water to

bringout the traces of pollutants. The resultant solution was centrifuged and the final product in the form of paste was extracted. Further, to remove moisture the precipitate was dried at 80 ℃ in a hot air oven for 1 hour and then annealed at 350 ℃ for 60min. Finally, black participates are collected and used for further investigations. The same investigation was repeated with same temperature but with different annealing time (90min and 120min) to study the effect of annealing time in the properties of CZTS nanoparticles. The samples annealed at 60min, 90min, and 120min are named as CZTS/60, CZTS/90 and CZTS/120 respectively.

Formation of CZTS nanoparticle has taken place according to the given reaction mechanism.

$$CuCl_2 \longrightarrow Cu^{2+} + 2Cl^-$$
$$ZnCl_2 \longrightarrow Zn^{2+} + 2Cl^-$$
$$SnCl_2 \longrightarrow Sn^{2+} + 2Cl^-$$
$$(NH_2)_2CS \longrightarrow NH_2\text{-}C^+\text{=}NH + H + S^{2-}$$

The final ionic reaction is

$$2Cu^{2+} + Zn^{2+} + Sn^{2+} + 4S^{2-} \longrightarrow Cu_2ZnSnS_4$$

The stoichiometric reaction for the formation of Cu_2ZnSnS_4

$$2CuCl_2.2H_2O + ZnCl_2 + SnCl_2.2H_2O + 4(NH_2)_2CS + 8H_2O \longrightarrow Cu_2ZnSnS_4 + 8NH_4 + 4CO_2$$

2.3. Characterization Techniques

Crystallinity and the orientation of Cu_2ZnSnS_4 nanoparticles are assessed by X-Ray Diffraction (XRD) technique by using an XPERT-PRO X-ray diffractometer with CuK radiation of =1.5406 Å. Horiba Jobin Yvon LABRAM – HR 800 spectrometer was used to record Raman spectrum. Surface morphology and compositional analysis of the CZTS nanoparticles are examined by scanning electron microscope(JEOL mode JSM 6390 SEM) equipped with the energy dispersive X-ray spectrometer (EDX). Shimadzu FT-IR with ATR Spectrometer was employed to measure the IR spectrum of the sample over the range of 400 to 4000 cm^{-1}. The absorption spectra of the sample are measured by using the JASCO Corp., V-570 spectrophotometer.

2.4. Preparation of photocathode

The CZTS photocathode was fabricated by the following procedure: the substrate (FTO glass plate) was washed with a mixed solution in the volume ratio 1:1:1 of deionized water, acetone, and ethanol for 10 min using ultrasonication. CZTS paste was prepared by dissolving the CZTS powder (2g) in ethylene glycol at room temperature. The mixture was then sonicated for 1 hour for homogeneous dispersal. CZTS nanoparticle paste was deposited on FTO glass plate using facile, cost-effective spin coating technique at 1500rpm for 30 sec. After that, the thin film was dried at 100 °C in a hot air oven for a half an hour with a four cycle of deposition and drying. Finally, the CZTS nanoparticle thin films are annealed at 350 °C for 1hour using a muffle furnace.

2.5. Photoelectrochemical water splitting experiment

Photoelectrochemical (PEC) characterisations are performed in an electrochemical workstation (Biologic 150, France) by using a single compartment cell with a three-electrode configuration. The prepared CZTS photocathode is used as a working electrode and counter electrode is a Pt wire and reference electrode is Ag/AgCl in saturated KCl, in the presence of Na_2SO_4 (pH=8) aqueous electrolyte of 0.5M. The light source used for PEC measurements is Xenon light source of 150W (GLORIA-X150A) attached with an AM 1.5 G filter. The distance between the light source and samples are adjusted to fix the light irradiation as 100 mW cm^{-2} (1 sun) at the surface of the photocathode. The applied potential (V) vs Ag/AgCl electrode was reported in case of reversible hydrogen electrode (RHE) using the formula [18]

$$E_{RHE} = E_{(Ag/AgCl)} + E^{\circ}_{(Ag/AgCl)} + 0.059pH \qquad (1)$$

$E^{\circ}_{(Ag/AgCl)} = 0.1976V$ at 25°C is the correction factor for reference electrode and $E_{(Ag/\ AgCl)}$ is the measured potential against the Ag/AgCl reference.

3. RESULTS AND DISCUSSION

3.1. X-ray diffraction (XRD) studies

X-ray Diffraction is used as the major tool for the identification of the phase purity and crystallinity of CZTS nanoparticles. The Crystalline or Grain size of the prepared CZTS samples was confirmed through the powder XRD technique using CuKα radiation. Figure.1 (a) shows the XRD pattern of CZTS nanoparticles annealed at 350 °C with different annealing times (60min, 90min and 120 min). The diffraction peaks are observed at 2θ =28.51°, 32.65°, 47.62°, 56.34° corresponding to (112), (200), (220) and (303) planes respectively for CSTS/60, CZTS/90 and CZTS/120. One additional peak at 40.48°

corresponds to (114) plane is observed for the sample annealed at 120 min. The diffraction peaks perceived can be indexed to tetragonal kesterite structure of CZTS. The peaks observed are in accordance with the standard JCPDS data: 26-0575 [19] of kesterite CZTS structure. The peaks corresponding to binary phases like Cu_2S, ZnS and ternary phases like Cu_2SnS_3, Cu_3SnS_4 are not present in the XRD pattern indicates the formation of Cu_2ZnSnS_4 only. The intense and sharp peaks of the samples show the good crystallinity of nanoparticles.

The Crystalline size of CZTS nanoparticles was estimated by using the Scherer's formula [20],

$$\mathbf{D=\frac{K\lambda}{\beta Cos\theta}(nm)} \qquad (2)$$

Where k is the shape factor (k=0.94), □ is the wavelength of CuK□1 radiation source =1.5406Å, □ is the peak width (Full Width Half Maximum) and □ is the Bragg angle.

The number of defects in the crystal was determined by using dislocation density (δ) and can be calculated by using the formula [21],

$$\boldsymbol{\delta} = \frac{\mathbf{1}}{\boldsymbol{D^2}} \text{ (lines/m}^2\text{)} \qquad (3)$$

Microstrain of the CZTS nanoparticles can be estimated by using the relation [21],

$$\boldsymbol{\varepsilon} = \frac{\boldsymbol{\beta \cos \theta}}{4} \qquad (4)$$

where □ is the peak width (Full Width Half Maximum) and □ is the Bragg angle. The lattice parameters of the tetragonal crystal system are calculated using the relation [21],

$$\frac{\mathbf{1}}{\boldsymbol{d^2}} = \frac{\boldsymbol{(h^2+k^2)}}{\boldsymbol{a^2}} + \frac{\boldsymbol{l^2}}{\boldsymbol{c^2}} \qquad (5)$$

Where d is the inter planar spacing, h,k,and l are the Miller indices and a, c are lattice constants. Cell volume can be calculated by the formula,

$$v = a^2 c \qquad (6)$$

The calculated Crystallite size **(D)**, Dislocation density **(δ)**, Strain **(ε),** Lattice parameters **(a),(c)** and Cell volume **(v)** are displayed in table.1.

Table. 1: Structural parameters of CZTS nanoparticles annealed at 350 °C with various annealing time

Annealing Time	Grain size D (nm)	MicroStrain ε x10^{-3}	Dislocation Density (δ) x10^{15} (lines/m^2)	a (nm)	c (nm)	Cell Volume v (Å^3)
60 min	23.36	1.497	1.878	0.549	1.060	319
90 min	27.78	1.265	1.349	0.543	1.090	322
120 min	30.44	1.148	1.103	0.546	1.089	326

The average crystallite size of CZTS nanoparticles was found to be 23-30 nm. Crystallite size are increased with the increase of annealing time as 23.36nm, 27.78nm and 30.44nm for CZTS/60, CZTS/90 and CZTS/120 respectively. The increase in crystallite size has an advantage for the photovoltaic and photocatalytic applications, as the photogenerated

electron-hole recombination rate would be reduced with large agglomerated grains. Hassanien et al.,[22] reported the increase in crystallite size value from 4.5nm to 38.8nm for CZTS with an annealing temperature of 400 ℃ to 550 ℃, Liping Chen et al.,[23] observed the increase in crystallite size from 5.60nm to 19.97nm in CZTS when annealed from 250 ℃ to 550 ℃, Giedrė Grincienė et al., [24] reported the size of crystallites increases from 2.4 to 24.1 nm for CZTS with the increase of annealing temperature from 300 ℃ to 550 ℃. The decrease in microstrain and dislocation density with an increase in crystallite size implies a less number of lattice defects i.e. good crystallinity. The lattice parameters calculated are in good concurrence with the report of Kishore et al., [25] and Mali et al.,[26] and also matched with standard JCPDS data (26-0575).

3.2. Raman analysis

Raman spectrum is a very sensitive tool for phase identification often combined with XRD results. The phase purity of the CZTS nanoparticles was determined using the Raman spectrum i.e. the existence of other phases, such as binary and ternary phases in CZTS nanoparticles will be investigated in detail using Raman spectra. The Raman spectrum of the CZTS nanoparticles for different annealing times is shown in figure.1 (b). The main peak at 339cm^{-1} along with small peak at 289cm^{-1} was observed for the samples annealed at 60 min and 90 min. The sample annealed at 90 min was observed the main peak at 339cm^{-1} along with shoulder peaks at 289cm^{-1}, 362cm^{-1}. The peaks are perfectly matched with the main Raman peaks of CZTS nanoparticles, which are close to the earlier reported values of CZTS of Kannan et al.,[27], Mkawi et al., [28], Jing Wang et al., [29]. The major peaks are recognised as the main vibrational A1 symmetry modes from the kesterite CZTS nanocrystals [30]. There are no signs of extra peaks related to the presence of secondary and ternary phases. Moreover, the intense major peak indicates the good crystalline quality of the sample. The results observed from Raman spectra are agreed with the XRD results.

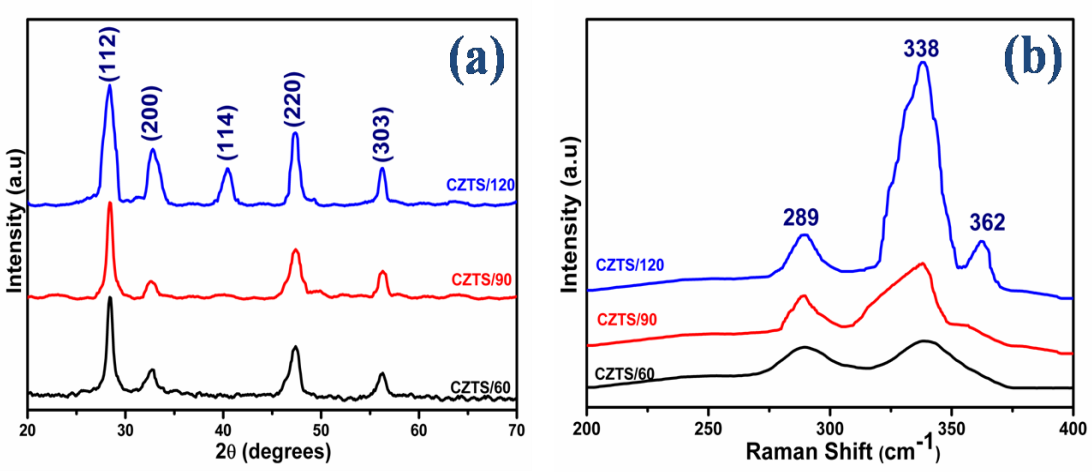

Figure. 1(a).XRD patterns 1(b). Raman spectra of CZTS nanoparticles annealed at 350 °C with different annealing times

3.3. Morphological analysis

Scanning electron microscope was used to examine the surface morphology of CZTS nanoparticles. Figure.2 shows the SEM image of CZTS nanoparticles prepared with different annealing times. The sample annealed at 60 min is agglomerated which is due to adhesion of particles to each other by weak forces leading to entities or structures of micrometer range. The sample annealed at 90 min composed of different types of shapes plates, polygons, etc. 2-D Nanoplate structure [31] is obtained for the sample annealed 120 min. An increase in annealing time induces a change in morphology from agglomerated form to nanocrystallites and then to nanoplates which arises as a result of covalent bond breaking between the molecules that are observed in the earlier stage of annealing (60 min).

3.4. Compositional analysis

The elemental composition of the CZTS was analyzed using the EDAX technique. This is used to confirm the existence of Copper, Zinc, Tin, and Sulfur. Figure 2 shows the EDAX spectrum of Cu_2ZnSnS_4 nanoparticles annealed at different time. It shows the presence of Cu, Zn, Sn and S in the stoichiometric ratio of 2:1:1:4. The atomic percentages of Cu:Zn:Sn:S is 26.39 : 13.80 : 14.12 : 45.69 for CZTS/60, 26.09 : 13.20 : 13.81 : 46.90 for CZTS/90 and 25.94 : 12.90 : 13.14 : 48.02 for CZTS/120. The absence of impurities such as C, O and Cl indicates the purity of the prepared samples. A kesterite structure of CZTS with no secondary phases was identified from EDAX agreed with the results of XRD and Raman spectra.

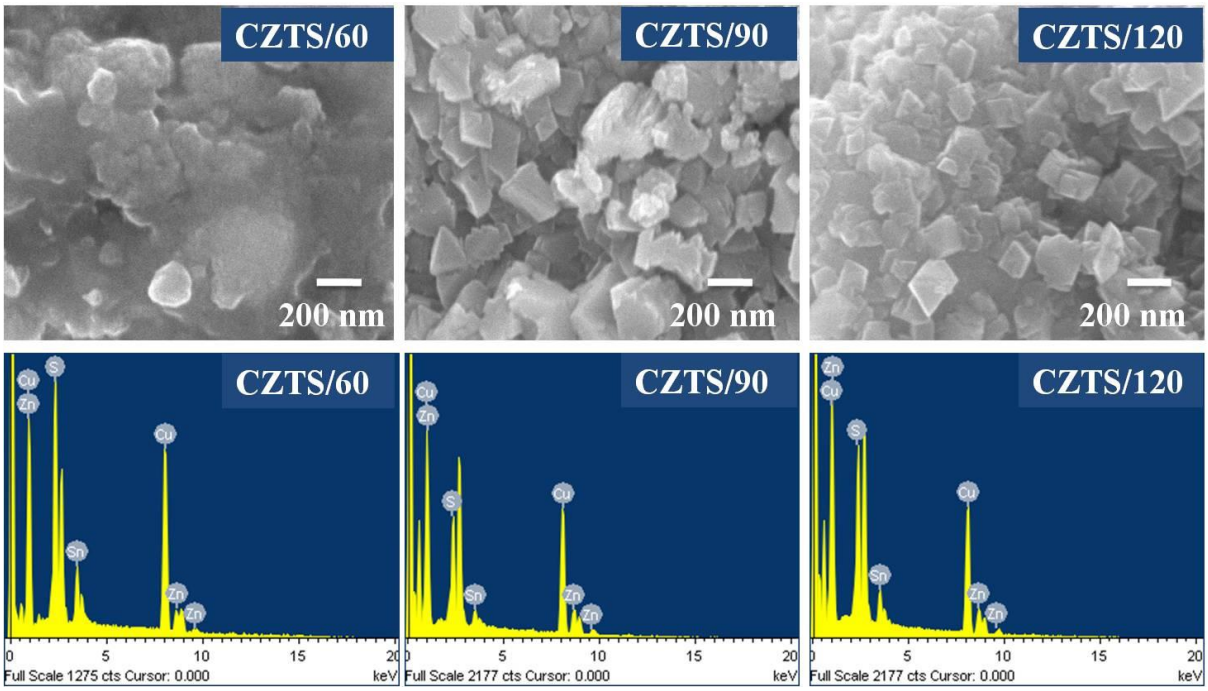

Figure. 2. SEM Images and EDAX spectra of CZTS nanoparticles annealed at 350 °C with different annealing times

3.5. FTIR studies

The impact of annealing time on the vibrational modes of Copper, Zinc, Tin, and Sulfur was investigated using an FTIR spectrophotometer. FTIR spectra of CZTS nanoparticles annealed at different times is shown in figure.3 The stretching and bending of oxygen was observed around 900–1600 cm^{-1}. The peak at 626 and 664 cm^{-1} is assigned to the ZnS band. The presence of sulphide ions in vibrational modes are observed as broad bands around 858 - 893 cm^{-1} [32]. The peak observed around 1050-1100 cm^{-1} and 1400-1460 cm^{-1} is due to NH_2 vibrational mode of thiourea. The peaks at 2980, 2928, and 2980 cm^{-1} are ascribed to the S–H thiol functional group and N-C-N stretching respectively [33]. The stretching of S-H bond is revealed by the peaks at 2350 and 2990 cm^{-1} respectively [34]. Presences of water, as well as thiourea are observed in the range of 3550-3750 cm^{-1} [32]. As a common observation, the shifts indicate a rearrangement of the CZTS network toward that of the stoichiometric structure with a lower structural disorder which gives rise to 2-D nanoplate morphologies witnessed in SEM analysis.

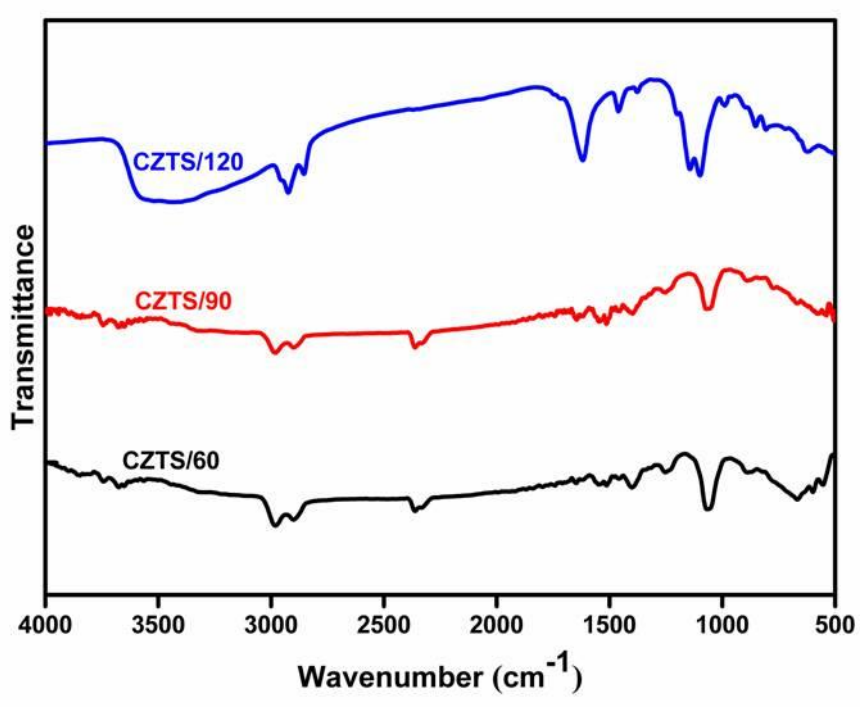

Figure. 3 FTIR spectra of CZTS nanoparticles annealed at 350 °C with different annealing times

3.6. UV analysis

*T*o study the optical absorption spectra and bandgap energy of the CZTS nanoparticles, absorption spectra are studied using UV–visible spectra in the wavelength range of 300 - 800 nm. The optical absorbance CZTS nanoparticles annealed at 350 °C with annealing time of 60min, 90min, and 120min are shown in the figure.4(a). It is clearly noticeable from the figure, all samples showed absorption in the visibe region.The spectra revealed that CZTS nanoparticles annealed with 120 min, indicating applicability as an absorbing material compared to 60min and 90min. Therefore, CZTS nanoparticles annealed at 350 °C with an annealing time of 120min is considered to be a suitable material for solar energy conversion.

Tauc and Davise Mott model was used to determine the optical bandgap energy E_g as a function of photon energy hν, by using the formula [35],

$$\boldsymbol{\alpha h\nu = A(h\nu - Eg)^n} \qquad (6)$$

where α- Absorption coefficient, hν - Incident photon energy, A- Constant, E_g - Bandgap energy, and n is index characterising the nature of optical transition i.e. for direct allowed transition n takes a value of 1/2 and for an indirect allowed transition n takes a of value 2.

Figure. 4(b) shows the Tauc plot of CZTS nanoparticles annealed at 350 ℃ with an annealing time of 60min, 90min, and 120min. The band gaps (E_g) are estimated to be 1.54eV, 1.50eV, and 1.48eV for 60min, 90min, and 120min respectively. The decrease in bandgap with increase in annealing time demonstrates less crystal defects with good crystalline quality. With the increasing of annealing time from 60min to 120 min, the bandgap decreased indicates that, the grain size increase may increase the absorbance nature of materials. The obtained band gap value is agreed upon with the earlier reports [36], [37], [38]. The bandgap observed is near the optimum value for photocatalytic and photovoltaic applications.

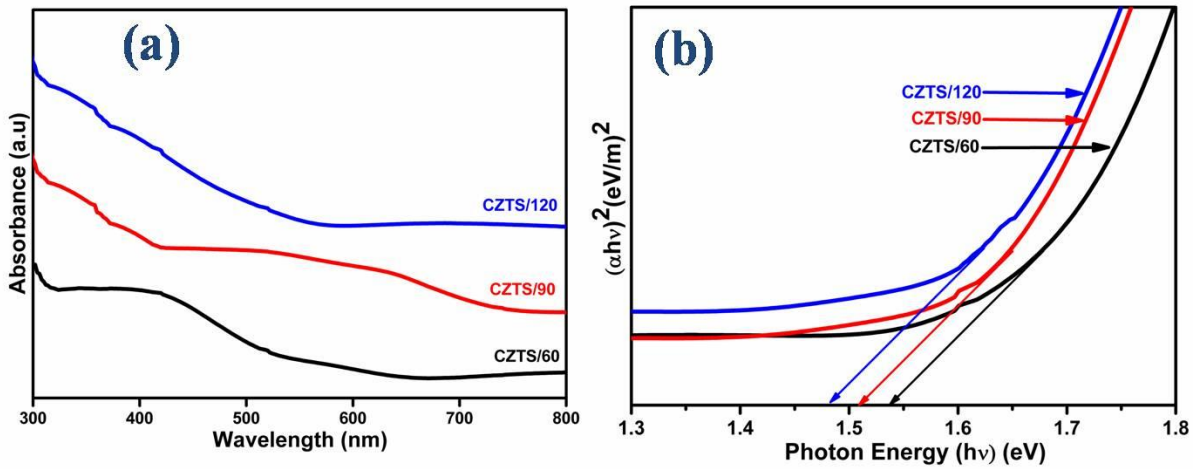

Figure. 4(a)UV Visible absorption spectra 4(b).Tauc plot of CZTS nanoparticles annealed at 350 °C with different annea

3.7. Photoelectrochemical properties

Photocurrent density generated by photocathode was measured to study its photoactivit , while the photocathode is dipped within the electrolyte solution. Figure 5(a) represents the LSV of CZTS photocathodes annealed at 350 ℃ with an annealing time of 60min, 90min, 120min. The current density under illumination represents the solar energy converted into electrical energy which is stored as chemical energy in the electrochemical cell. The direction of photocurrent is expected behaviour for p-type semiconductor, where electron injection towards the electrolyte while holes travel towards the counter electrode via an external circuit. The charge accumulation on the semiconductor is due to the rapid increase in cathodic current, which gives rise to an exponential capacity [39]. It can be noticed from LSV curve, all the photocathodes exhibit improved photocurrent density upon illumination. The enhancement of photocurrent exhibits the light-sensitive nature of CZTS material. The photocurrent density value increases very small with the increase in annealing time from 60 min to 120 min.

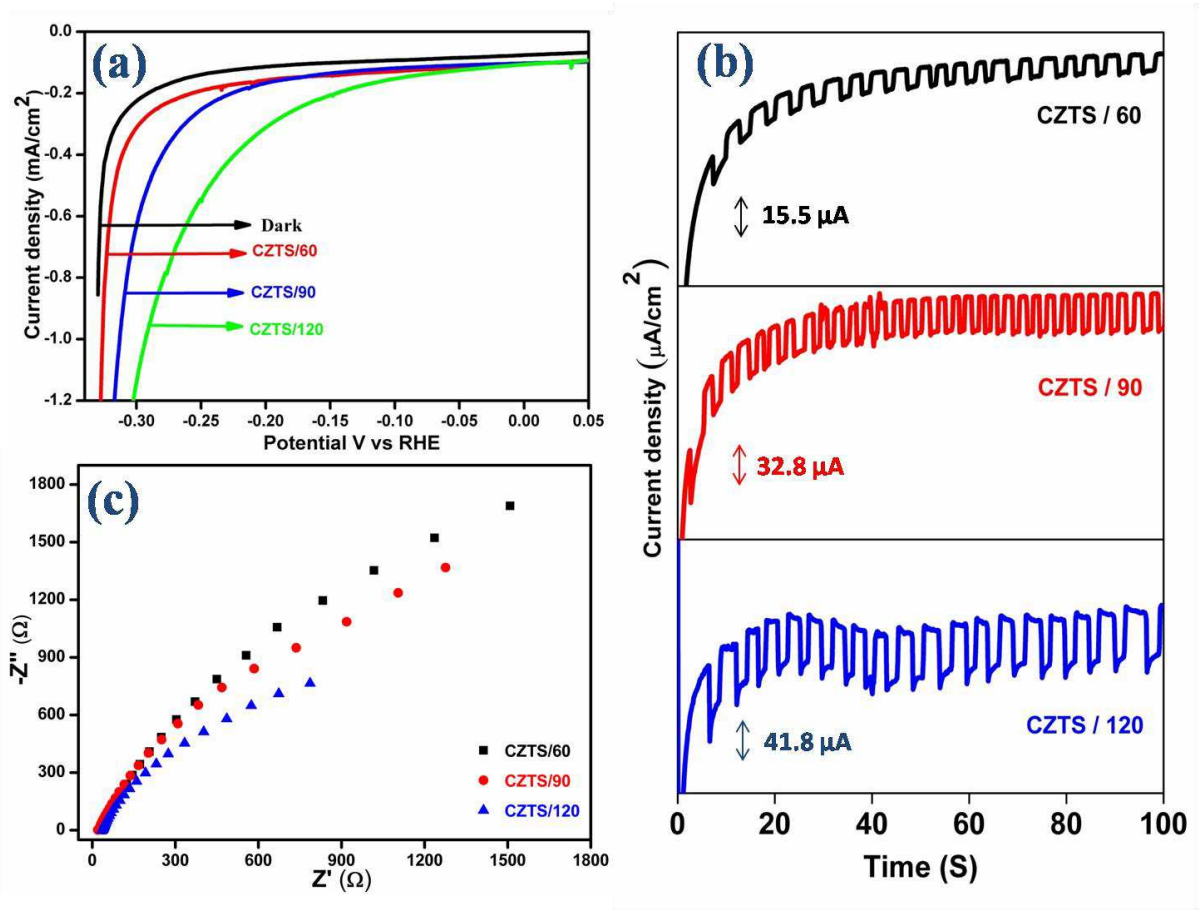

Figure. 5(a) Linear sweep voltammetry (b). *i-t* curves (c) Nyquist plot of CZTS at 350 °C with different annealing times

Chronoamperometry measurements are carried out at 1sun (100 mW cm^{-2}) illuminations under chopped light illumination conditions in 0.5M Na_2SO_4 (pH=8) aqueous solution for CZTS/60, CZTS/90, and CZTS/120 photocathodes. Figure 5(b) represents the i-t curves of CZTS photocathodes annealed at 350 °C with an annealing time of 60min, 90min, 120min. The results from the i-t curves showed a stable photoresponse in the aqueous Na_2SO_4 solution for all the electrodes. As shown in figure 5(b), CZTS/120 photocathode represents higher photocurrent density (41.8 µA/cm^2) than CZTS/60 (32.8 µA/cm^2) and CZTS/120 (15.5 µA/cm^2) was obtained at 0V (vs RHE). The increasing photocurrent density of prepared photocathodes was revealed that the increase of their corresponding annealing time. The obtained morphology (2-D nanoplate) gives good interfacial contact between the material and electrolyte thus offering improved photocurrent density. The photo-activity of the CZTS thin film was confirmed from photoelectrochemical measurement, which was already confirmed in UV–visible spectra.

3.7.1.Electrochemical Impedance Spectroscopy Analysis

Electrochemical Impedance Spectroscopy (EIS) is used for a better understanding of electrochemical activity. EIS spectra of CZTS photocathodes are shown in figure 5(c). From figure 5(c), the semicircle of all the CZTS electrodes annealed at 350°C with a different annealing times, the plot becomes narrower strategy. The lower semicircle indicates a higher conductivity and increase of charge transfer resistance due to the increase of annealing time, which enabled electrodes activation; the results could be better PEC performance.

4. Conclusion

Cu_2ZnSnS_4 (CZTS) nanoparticles are successfully synthesized by simple one-step chemical method with post-annealing in air at different annealing time and with an annealing temperature of 350°C. The results of XRD and Raman spectrum confirm the formation of tetragonal kesterite structure of CZTS nanoparticles with good crystallinity and absence of secondary phases. Moreover, the grain size of the CZTS nanoparticles had a substantial growth when the annealing time was increased from 60 minutes to 120 minutes. The 2-D nanoplate morphology is obtained for the sample annealed at 350°C with an annealing time of 120 minutes. The chemical composition of the CZTS nanoparticles is near the stoichiometric ratio. FT-IR spectra confirms the presence of functional group present in the CZTS samples. Optical measurements show that the direct bandgap of the CZTS nanoparticles at different annealing time decreased from 1.54 eV to 1.48 eV. Moreover, the nanoparticle thinfilms was prepared to study the water splitting performance. The CZTS/120 photocathode exhibited higher photocurrent density when compared with other two photocathodes because of larger grain size the recombination of electron-hole pairs at the grain boundaries was reduced. The enhancement in the cathodic photocurrent density of CZTS/120 during the water-splitting process was due to the lower bandgap and higher electrical conductivity of the sample.

References

[1] C. Sripan, V.E. Madhavan, A.K. Viswanath, R. Ganesan, Sulfurization and annealing effects on thermally evaporated CZTS films, Mater. Lett. 189 (2017) 110–113. https://doi.org/10.1016/j.matlet.2016.11.094.

[2] J. Li, N. Wu, Semiconductor-based photocatalysts and photoelectrochemical cells for solar fuel generation: A review, Catal. Sci. Technol. 5 (2015) 1360–1384.

https://doi.org/10.1039/c4cy00974f.

[3] Y. Chen, X. Feng, M. Liu, J. Su, S. Shen, Towards efficient solar-to-hydrogen conversion: Fundamentals and recent progress in copper-based chalcogenide photocathodes, Nanophotonics. 5 (2016) 468–491. https://doi.org/10.1515/nanoph-2016-0027.

[4] C.K. Sumesh, S.C. Peter, Two-dimensional semiconductor transition metal based chalcogenide based heterostructures for water splitting applications, Dalt. Trans. 48 (2019) 12772–12802. https://doi.org/10.1039/c9dt01581g.

[5] C. Ros, T. Andreu, J.R. Morante, Photoelectrochemical water splitting: a road from stable metal oxides to protected thin film solar cells, J. Mater. Chem. A. 8 (2020) 10625–10669. https://doi.org/10.1039/d0ta02755c.

[6] N.K. Awad, E.A. Ashour, N.K. Allam, Recent advances in the use of metal oxide-based photocathodes for solar fuel production, J. Renew. Sustain. Energy. 6 (2014). https://doi.org/10.1063/1.4871899.

[7] Q. Huang, Z. Ye, X. Xiao, Recent progress in photocathodes for hydrogen evolution, J. Mater. Chem. A. 3 (2015) 15824–15837. https://doi.org/10.1039/c5ta03594e.

[8] A.I. Inamdar, K.Y. Jeon, H.S. Woo, W. Jung, H. Im, H. Kim, Controlled growth of Cu 2ZnSnS 4 (CZTS) thin films for heterojunction solar-cell applications, J. Korean Phys. Soc. 60 (2012) 1730–1734. https://doi.org/10.3938/jkps.60.1730.

[9] K.S. Lim, S.M. Yu, A.R. Khalkar, T.S. Oh, J. Nam, D.W. Shin, J.B. Yoo, Comparison of Cu2ZnSnS4 thin films and solar cell performance using Zn target with ZnS target, J. Alloys Compd. 650 (2015) 641–646. https://doi.org/10.1016/j.jallcom.2015.08.056.

[10] J. Tao, J. Liu, J. He, K. Zhang, J. Jiang, L. Sun, P. Yang, J. Chu, Synthesis and characterization of Cu2ZnSnS4 thin films by the sulfurization of co-electrodeposited Cu-Zn-Sn-S precursor layers for solar cell applications, RSC Adv. 4 (2014) 23977–23984. https://doi.org/10.1039/c4ra02327g.

[11] K. Muska, M. Kauk, M. Altosaar, M. Pilvet, M. Grossberg, O. Volobujeva, Synthesis of Cu 2ZnSnS 4 monograin powders with different compositions, Energy Procedia. 10 (2011) 203–207. https://doi.org/10.1016/j.egypro.2011.10.178.

[12] D.C. Nguyen, S. Ito, D.V.A. Dung, Effects of annealing conditions on crystallization of the CZTS absorber and photovoltaic properties of Cu(Zn,Sn)(S,Se)2 solar cells, J. Alloys Compd. 632 (2015) 676–680. https://doi.org/10.1016/j.jallcom.2015.01.258.

[13] E. Kask, T. Raadik, M. Grossberg, R. Josepson, J. Krustok, Deep defects in Cu 2ZnSnS 4 monograin solar cells, Energy Procedia. 10 (2011) 261–265.

https://doi.org/10.1016/j.egypro.2011.10.188.

[14] M. Jeon, Y. Tanaka, T. Shimizu, S. Shingubara, Formation and characterization of single-step electrodeposited Cu 2ZnSnS 4 thin films: Effect of complexing agent volume, Energy Procedia. 10 (2011) 255–260. https://doi.org/10.1016/j.egypro.2011.10.187.

[15] H. Zhou, W.C. Hsu, H.S. Duan, B. Bob, W. Yang, T. Bin Song, C.J. Hsu, Y. Yang, CZTS nanocrystals: A promising approach for next generation thin film photovoltaics, Energy Environ. Sci. 6 (2013) 2822–2838. https://doi.org/10.1039/c3ee41627e.

[16] D. Yokoyama, T. Minegishi, K. Jimbo, T. Hisatomi, G. Ma, M. Katayama, J. Kubota, H. Katagiri, K. Domen, H2 evolution from water on modified Cu2ZnSnS 4 photoelectrode under solar light, Appl. Phys. Express. 3 (2010). https://doi.org/10.1143/APEX.3.101202.

[17] Y. Zhang, S. Ouyang, Q. Yu, P. Li, J. Ye, Modulation of sulfur partial pressure in sulfurization to significantly improve the photoelectrochemical performance over the Cu2ZnSnS4 photocathode, Chem. Commun. 51 (2015) 14057–14059. https://doi.org/10.1039/c5cc04812e.

[18] K. Ramachandran, M. Geerthana, P. Maadeswaran, B. Liang, R. Ramesh, Enhanced photoelectrochemical water splitting performance of hematite photoanodes by hybrid microwave annealing process, Optik (Stuttg). 212 (2020) 164658. https://doi.org/10.1016/j.ijleo.2020.164658.

[19] L. Dong, S. Cheng, Y. Lai, H. Zhang, H. Jia, Sol-gel processed CZTS thin film solar cell on flexible molybdenum foil, Thin Solid Films. 626 (2017) 168–172. https://doi.org/10.1016/j.tsf.2017.02.019.

[20] N.M. Shinde, D.P. Dubal, D.S. Dhawale, C.D. Lokhande, J.H. Kim, J.H. Moon, Room temperature novel chemical synthesis of Cu 2ZnSnS 4 (CZTS) absorbing layer for photovoltaic application, Mater. Res. Bull. 47 (2012) 302–307. https://doi.org/10.1016/j.materresbull.2011.11.020.

[21] M.J. Chithra, M. Sathya, K. Pushpanathan, Effect of pH on crystal size and photoluminescence property of zno nanoparticles prepared by chemical precipitation method, Acta Metall. Sin. (English Lett. 28 (2015) 394–404. https://doi.org/10.1007/s40195-015-0218-8.

[22] A.E. Hassanien, S. Abdelhaleem, R. Ahmad, M. Schuster, S.H. Moustafa, M. Distaso, W. Peukert, P.J. Wellmann, Effect of Fast Annealing on Structural Characteristics and Optical Properties of Cu 2 ZnSnS 4 Absorber Films Deposited by Doctor-Blade

Technique , J. Nanoelectron. Optoelectron. 14 (2019) 1394–1400. https://doi.org/10.1166/jno.2019.2633.

[23] L. Chen, C. Park, Effects of annealing temperature on Cu2ZnSnS4 (CZTS) films formed by electrospray technique, Korean J. Chem. Eng. 34 (2017) 1187–1191. https://doi.org/10.1007/s11814-017-0011-7.

[24] G. Grinciene, V. Pakštas, R. Giraitis, G. Niaura, A. Naujokaitis, J. Juodkazyte, L. Tamašauskaite-Tamašiunaite, R. Juškenas, B. Šimkunaite-Stanyniene, E. Norkus, Properties and characterization of CZTS nanoparticles prepared by microwave heating irradiation, Chemija. 29 (2018) 29–40. https://doi.org/10.6001/chemija.v29i1.3641.

[25] Y.B. Kishore Kumar, G. Suresh Babu, P. Uday Bhaskar, V. Sundara Raja, Preparation and characterization of spray-deposited Cu2ZnSnS4 thin films, Sol. Energy Mater. Sol. Cells. 93 (2009) 1230–1237. https://doi.org/10.1016/j.solmat.2009.01.011.

[26] S.S. Mali, P.S. Shinde, C.A. Betty, P.N. Bhosale, Y.W. Oh, P.S. Patil, Synthesis and characterization of Cu 2ZnSnS 4 thin films by SILAR method, J. Phys. Chem. Solids. 73 (2012) 735–740. https://doi.org/10.1016/j.jpcs.2012.01.008.

[27] A.G. Kannan, T.E. Manjulavalli, J. Chandrasekaran, Influence of Solvent on the Properties of CZTS Nanoparticles, Procedia Eng. 141 (2016) 15–22. https://doi.org/10.1016/j.proeng.2015.08.1112.

[28] E.M. Mkawi, Y. Al-Hadeethi, E. Shalaan, E. Bekyarova, Solution-processed sphere-like Cu2ZnSnS4 nanoparticles for solar cells: effect of oleylamine concentration on properties, Appl. Phys. A Mater. Sci. Process. 126 (2020) 2–9. https://doi.org/10.1007/s00339-019-3233-1.

[29] J. Wang, P. Zhang, X. Song, L. Gao, Surfactant-free hydrothermal synthesis of Cu2ZnSnS4 (CZTS) nanocrystals with photocatalytic properties, RSC Adv. 4 (2014) 27805–27810. https://doi.org/10.1039/c4ra03444a.

[30] D.B. Mohan, Impact of Annealing Temperature on the Phase of CZTS with the Variation in Surface Morphological Changes and Extraction of Optical Bandgap Impact of Annealing Temperature on the Phase of CZTS with the, (2017). https://doi.org/10.1088/1742-6596/755/1/011001.

[31] F. Mehmood, J. Iqbal, A. Gul, W. Ahmed, M. Ismail, Facile synthesis of 2-D Cu doped WO3 nanoplates with structural, optical and differential anti cancer characteristics, Phys. E Low-Dimensional Syst. Nanostructures. 88 (2017) 188–193. https://doi.org/10.1016/j.physe.2016.12.008.

[32] D.K. Maurya, S. Sikarwar, P. Chaudhary, S. Angaiah, B.C. Yadav, Synthesis and

Characterization of Nanostructured Copper Zinc Tin Sulphide (CZTS) for Humidity Sensing Applications, IEEE Sens. J. 19 (2019) 2837–2846. https://doi.org/10.1109/JSEN.2018.2890309.

[33] K. Rawat, P.K. Shishodia, Structural and optical properties of sol gel derived Cu2ZnSnS4 nanoparticles, Adv. Powder Technol. 28 (2017) 611–617. https://doi.org/10.1016/j.apt.2016.11.013.

[34] M. Patel, I. Mukhopadhyay, A. Ray, Structural, optical and electrical properties of spray-deposited CZTS thin films under a non-equilibrium growth condition, J. Phys. D. Appl. Phys. 45 (2012). https://doi.org/10.1088/0022-3727/45/44/445103.

[35] R.J. Deokate, A.D. Adsool, N.S. Shinde, S.M. Pawar, C.D. Lokhande, Structural and optical properties of spray-deposited Cu 2ZnSnS4 thin films, Energy Procedia. 54 (2014) 627–633. https://doi.org/10.1016/j.egypro.2014.07.304.

[36] B.L. Guo, Y.H. Chen, X.J. Liu, W.C. Liu, A.D. Li, Optical and electrical properties study of sol-gel derived Cu2ZnSnS4 thin films for solar cells, AIP Adv. 4 (2014) 0–10. https://doi.org/10.1063/1.4895520.

[37] A. Wangperawong, J.S. King, S.M. Herron, B.P. Tran, K. Pangan-Okimoto, S.F. Bent, Aqueous bath process for deposition of Cu2ZnSnS4 photovoltaic absorbers, Thin Solid Films. 519 (2011) 2488–2492. https://doi.org/10.1016/j.tsf.2010.11.040.

[38] S. Sarkar, K. Bhattacharjee, G.C. Das, K.K. Chattopadhyay, Self-sacrificial template directed hydrothermal route to kesterite-Cu 2ZnSnS4 microspheres and study of their photo response properties, CrystEngComm. 16 (2014) 2634–2644. https://doi.org/10.1039/c3ce42229a.

[39] J. Bisquert, F. Fabregat-Santiago, I. Mora-Seró, G. Garcia-Belmonte, E.M. Barea, E. Palomares, A review of recent results on electrochemical determination of the density of electronic states of nanostructured metal-oxide semiconductors and organic hole conductors, Inorganica Chim. Acta. 361 (2008) 684–698. https://doi.org/10.1016/j.ica.2007.05.032.

Figures

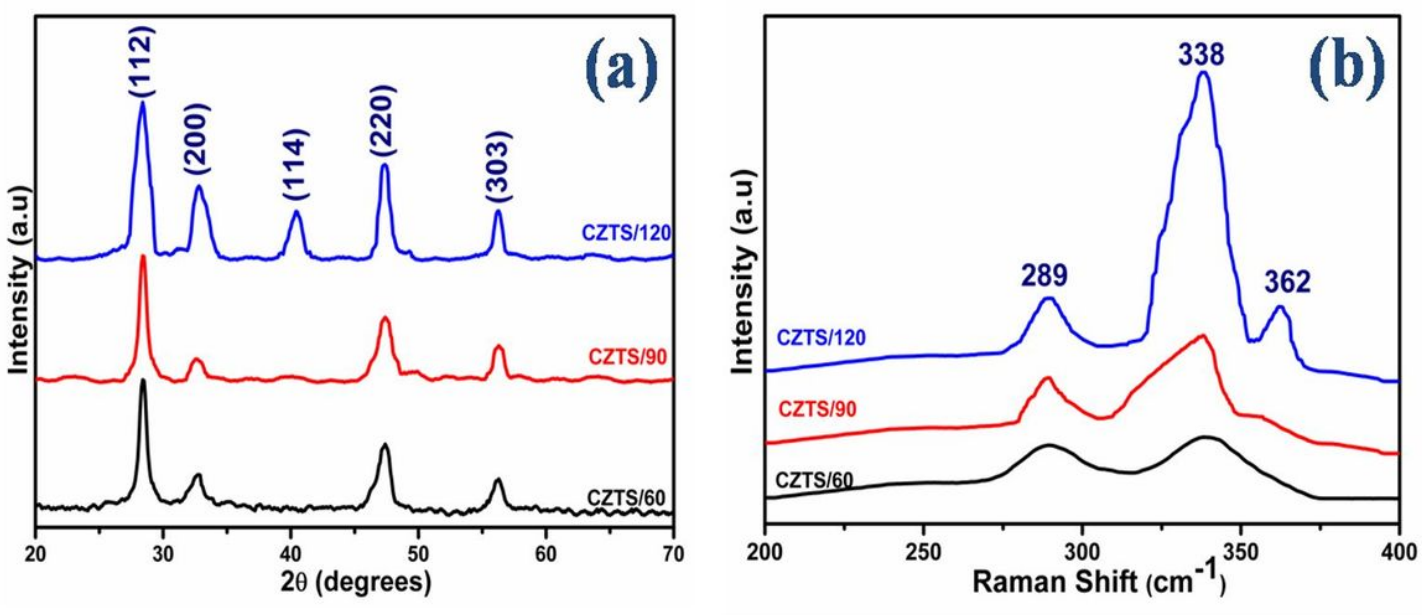

Figure 1

(a).XRD patterns 1(b). Raman spectra of CZTS nanoparticles annealed at 350 °C with different annealing times

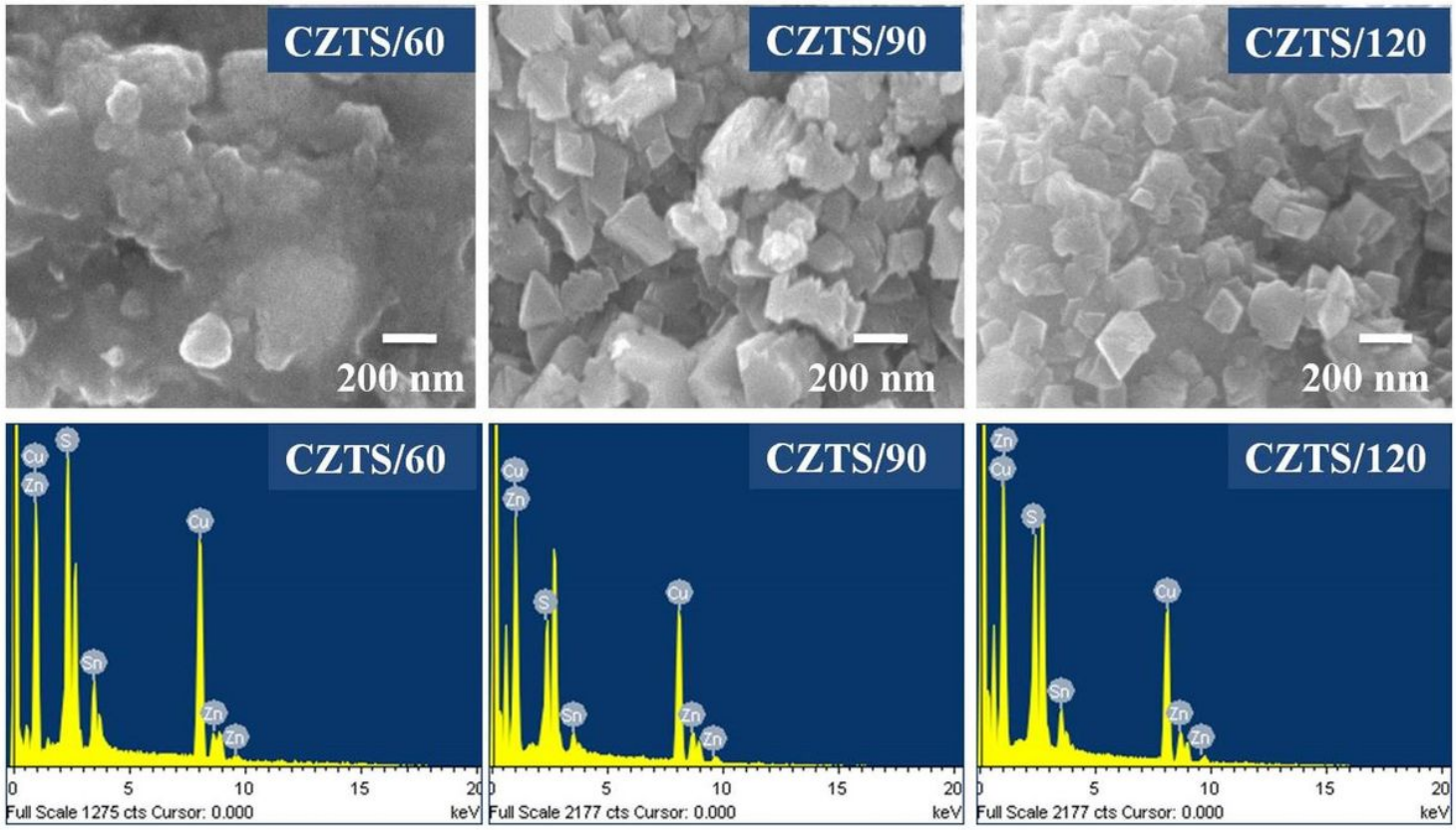

Figure 2

SEM Images and EDAX spectra of CZTS nanoparticles annealed at 350 °C with different annealing times

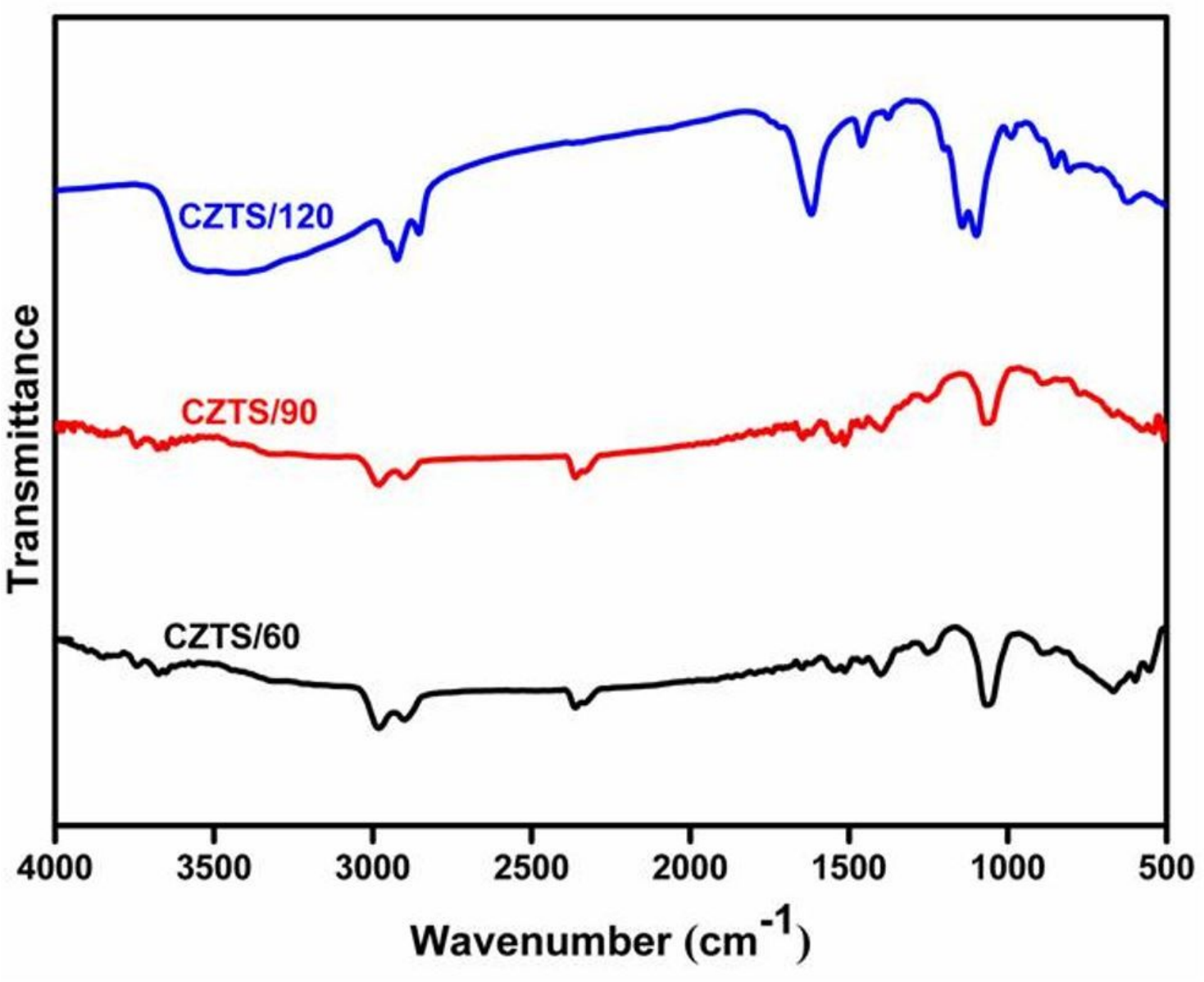

Figure 3

FTIR spectra of CZTS nanoparticles annealed at 350 °C with different annealing times

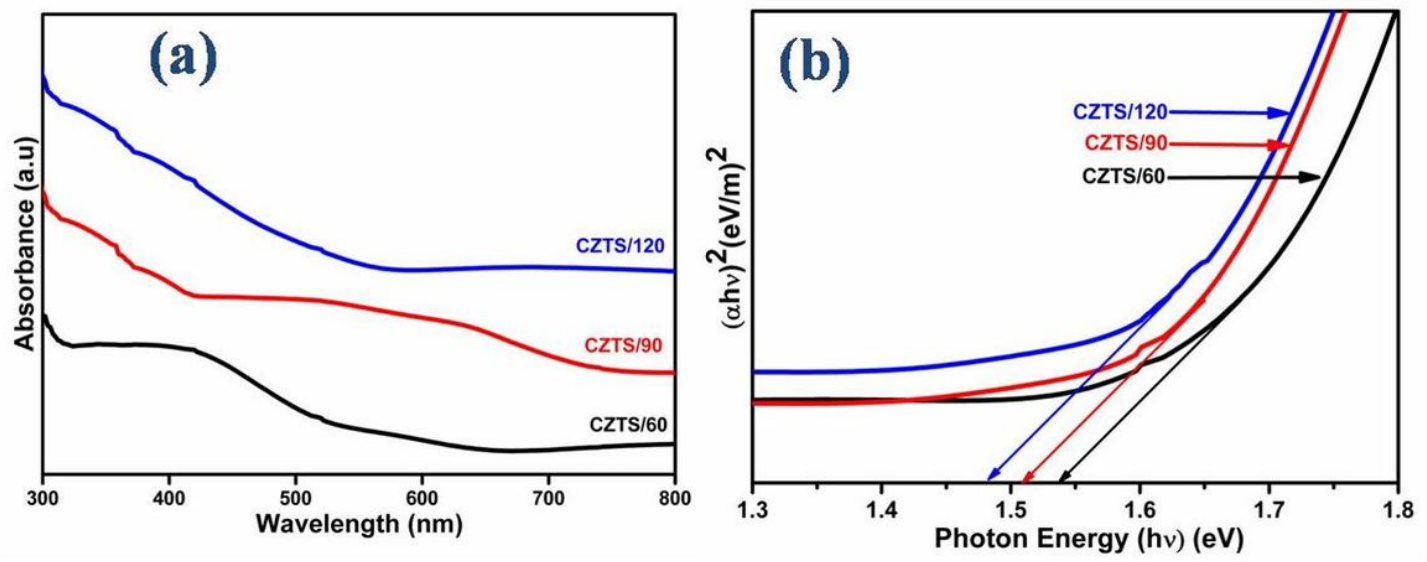

Figure 4

(a)UV Visible absorption spectra 4(b).Tauc plot of CZTS nanoparticles annealed at 350 °C with different annea

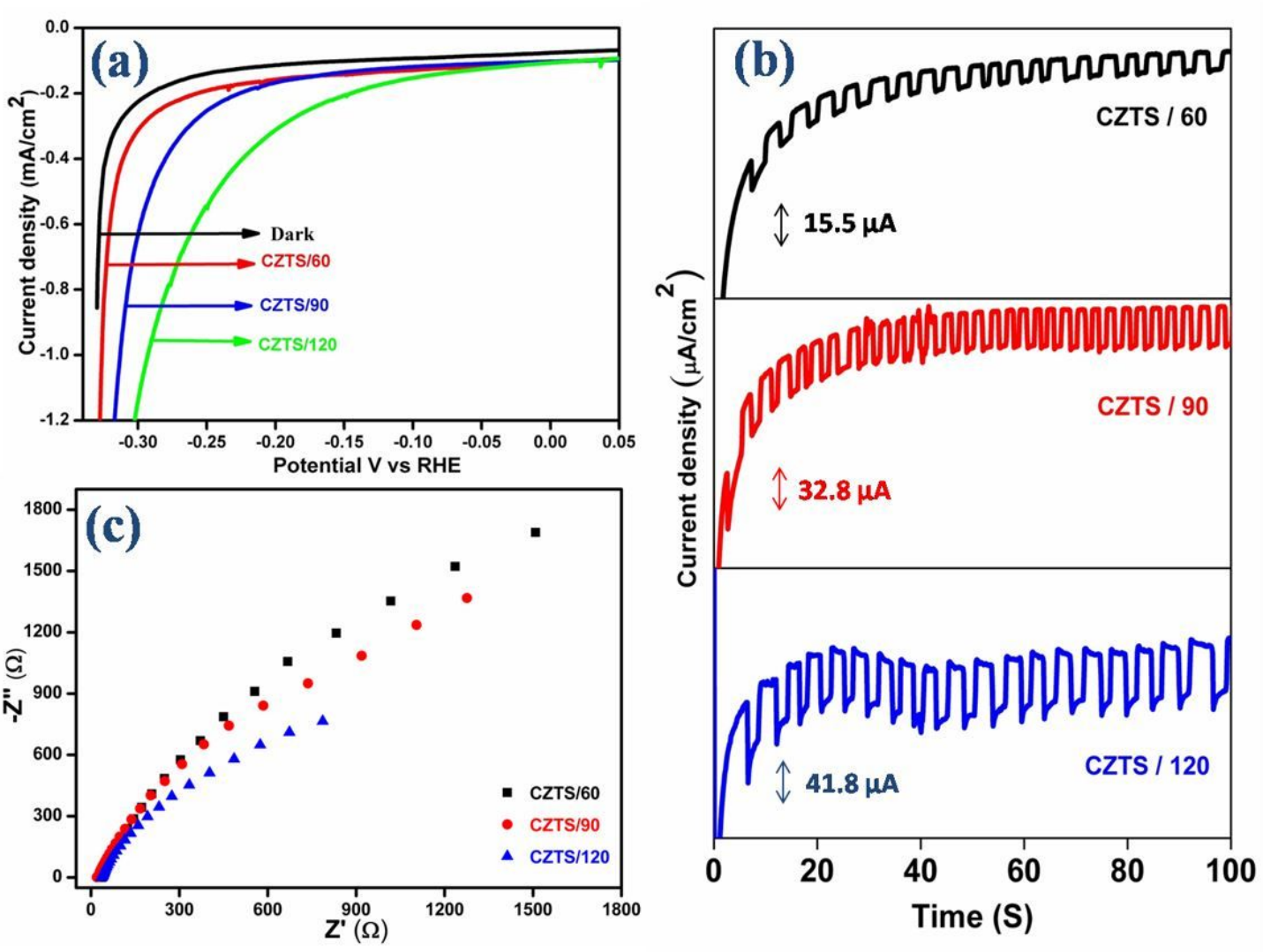

Figure 5

(a) Linear sweep voltammetry (b). i-t curves (c) Nyquist plot of CZTS at 350 °C with different annealing times